Research in Astron. Astrophys. **2010** Vol. **10** No. **5**, 427–437
http://www.raa-journal.org *http://www.iop.org/journals/raa*

Research in Astronomy and Astrophysics

The study of Seyfert 2 galaxies with and without infrared broad lines *

Hong-Bing Cai[1,2], Xin-Wen Shu[1], Zhen-Ya Zheng[1] and Jun-Xian Wang[1]

[1] CAS Key Laboratory for Research in Galaxies and Cosmology, Department of Astronomy, University of Science and Technology of China, Hefei 230026, China
[2] National Time Service Center, CAS, Xi'an 710600, China; *hbcai@ntsc.ac.cn*

Received 2009 December 17; accepted 2010 February 23

Abstract From the literature, we construct a sample of 25 Seyfert 2 galaxies (S2s) with a broad line region (BLR) detected in near infrared (NIR) spectroscopy and 29 with NIR BLRs which were not detected. We find no significant difference between the nuclei luminosity (extinction-corrected [OIII] 5007) and infrared color f_{60}/f_{25} between the two populations, suggesting that the non-detections of NIR BLRs could not be due to low AGN luminosity or contamination from the host galaxy. As expected, we find significantly lower X-ray obscurations in Seyfert 2s with NIR BLR detection, supporting the unification scheme. However, such a scheme was challenged by the detection of NIR BLRs in heavily X-ray obscured sources, especially in six of them with Compton-thick X-ray obscuration. The discrepancy could be solved by the clumpy torus model and we propose a toy model demonstrating that IR-thin X-ray-thick S2s could be viewed at intermediate inclinations and compared with those IR-thick X-ray-thick S2s. We note that two of the IR-thin X-ray-thick S2s (NGC 1386 and NGC 7674) experienced X-ray transitions, i.e. from Compton-thin to Compton-thick appearance or vice versa based on previous X-ray observations, suggesting that X-ray transitions could be common in this special class of objects.

Key words: galaxies: active — galaxies: Seyfert — infrared: galaxies

1 INTRODUCTION

Spectropolarimetric observations have detected hidden broad emission line regions in many Seyfert 2 galaxies (i.e., Antonucci & Miller 1985). This kind of S2s can be unified with Seyfert 1 galaxies (S1s) under the unification scheme (Antonucci 1993), in which the key component is a dusty torus surrounding the nucleus, and different lines of sight (obscured by the torus or not) induce different apparent properties between S1 and S2. Strong evidence supporting the unified model also comes from X-ray observations, which show that most S2s are generally heavily obscured ($N_{\rm H} > 10^{22}$ cm^{-2}) (Risaliti et al. 1999; Bassani et al. 1999). However, only $\sim$ 50% of S2s with spectropolarimetric observations show polarized broad emission lines (PBLs) in polarized spectra (e.g. Tran 2001). The visibility of PBLs was found to be dependent on many factors, including intrinsic AGN luminosity,

* Supported by the National Natural Science Foundation of China.

infrared colors, nuclei obscuration, and likely more, and provides valuable information on the physical properties and geometry of the obscuration, scattering region, and the broad emission line region (e.g., Shu et al. 2007 and references therein).

Another efficient way to detect the hidden broad line regions in S2s is near-infrared (NIR) spectroscopy, due to the relatively smaller dust opacity in NIR than in the optical (e.g. see Gordon et al. 2003 for a Galactic dust extinction curve). For instance, the Galactic dust extinction at 4.05 μm is ~ 20 times weaker than in the V band ($A_{4.05\,\mu\mathrm{m}}/A_V = 0.051$, Lutz 1999). NIR observations have succeeded in detecting NIR broad emission lines in some (but not all) S2s (e.g., Goodrich et al. 1994; Veilleux et al. 1997a; Lutz et al. 2002), providing further support to the AGN unification model. By studying a sample of 12 type 2 AGNs, Lutz et al. (2002) found all three objects with detected broad Brα lines exhibit relatively low X-ray obscuring columns ($N_{\mathrm{H}} < 10^{23}\,\mathrm{cm}^{-2}$), while those without are more heavily obscured in X-ray (with $N_{\mathrm{H}} > 10^{23}\,\mathrm{cm}^{-2}$). More interestingly, the NIR opacities they found were consistent with a Galactic ratio of 4 μm obscuration of the BLR and X-ray column.

However, careful examinations of other factors which could affect the visibility of NIR BLRs have not been performed, and better understanding of the relation between NIR and X-ray obscuration in Seyfert 2 galaxies demands larger samples. In this paper, we construct a large sample of S2s from the literature with detected NIR broad emission lines (IRBL S2s hereafter) and those which were not detected (non-IRBL S2s), and perform the first systematic comparison. Throughout this paper, we use the cosmological parameters H_0 =70 km s^{-1} Mpc^{-1}, $\Omega_{\mathrm{m}} = 0.27$, and $\Omega_\lambda = 0.73$.

2 SAMPLE AND STATISTICAL PROPERTIES

By searching the literature, we collected 25 IRBL S2s. We exclude intermediate Seyferts (Seyfert 1.8, Seyfert 1.9) which will otherwise bias our comparison of obscuration (see Sect. 3) since they were defined to be less obscured in the optical, and thus most of them are observable in the near infrared and X-ray. Most of these infrared broad lines are hydrogen recombination lines, i.e., Bracket and Paschen lines, except for one He I 10830 in NGC 1275. The sample and the detected NIR broad emission lines and widths are listed in Table 1. We also list the following in the table for each source: in Cols. (5)–(6) whether or not polarized broad emission lines were detected and their corresponding references; in Col. (7) IR flux density ratio $f_{60\,\mu\mathrm{m}}/f_{20\,\mu\mathrm{m}}$, where f_{60} and f_{20} are directly from NED except for Mrk 477 and 3C 223 whose values are obtained by interpolation or extrapolation according to their infrared spectrum; in Cols. (8)–(9) X-ray absorption column density and references; in Cols. (10)–(12) reddening-corrected [O III] line flux, luminosity and references. For comparison, we list the sample of 29 non-IRBL S2s in Table 2. LINERs are excluded from the sample.

When calculating the luminosity of [O III] in Tables 1 and 2, we have applied $F^{\mathrm{cor}}_{[\mathrm{O\ III}]} = F^{\mathrm{obs}}_{[\mathrm{O\ III}]}[(\mathrm{H}\alpha/\mathrm{H}\beta)_{\mathrm{obs}}/(\mathrm{H}\alpha/\mathrm{H}\beta)_0]^{2.94}$ (Bassani et al. 1999) to correct the dust extinction to [O III], where $F^{\mathrm{cor}}_{[\mathrm{O\ III}]}$ is the extinction-corrected flux of [O III] 5007, and $F^{\mathrm{obs}}_{[\mathrm{O\ III}]}$ the observed flux of [O III] 5007 with an intrinsic Balmer decrement of $(\mathrm{H}\alpha/\mathrm{H}\beta)_0 = 3.0$.

In Figure 1 we plot the redshift distribution of both IRBL S2s and non-IRBL S2s. Most of the sources are located at redshift < 0.05, except for several IRBL S2s. A K-S test shows that the redshift distributions of IRBL S2s and non-IRBL S2s are statistically different with a confidence level of 99.8%. We attribute this difference to the inhomogeneous nature of the samples (combined from the literature).

Various studies have found a higher detection rate of PBLs in S2s with higher AGN luminosity (see Shu et al. 2007 and references therein). To investigate whether the visibility of NIR broad emission lines in S2s depends on AGN's intrinsic luminosity, in Figure 2 we plot the histogram distribution of reddening-corrected $L_{[\mathrm{O\ III}]}$ for IRBL S2s and non-IRBL S2s. We find a weak trend that non-IRBL S2s show lower $L_{[\mathrm{O\ III}]}$, however, the difference is statistically insignificant (a K-S test shows that the difference only has a confidence level of 90%).

Table 1 Sample of Seyfert 2s with Near-infrared Broad Lines

Source	z	Width	Ref.	PBL	Ref.	f_{60}/f_{25}	$\log N_{\rm H}$	Ref.	$F_{[\rm O\ III]}$	$\log L_{[\rm O\ III]}$	Ref.
(1)	(2)	(3)	(4)	(5)	(6)	(7)	(8)	(9)	(10)	(11)	(12)
3C 223	0.14	Paα4100	H96	?	...	0.26	22.88	C04	3.88	42.28	P07
F13451+1232	0.12	Paα2588	V97b	?	...	2.88	22.65	I04	2.79	42.02	A00
F23498+2423	0.21	Paα3027	V97b	?	...	8.51	...	...	12.11	43.2	V99
F13305–1739	0.148	Paα2896	V99	?	...	2.95	...	...	361.96	44.33	V99
IRAS 08311–2459	0.10	Paα779	M00	?	...	4.53	...	...	...	...	...
IRAS 15462–0450	0.10	Paα	M99	?	...	6.48	...	...	6.15	42.19	V99
NGC 6240	0.024	Brα1800	S08	?	...	6.48	24.13	P03	135	42.27	B99
Arp 220	0.018	Brα3300	D87	?	...	13.01	22.48	C02	3.69	40.44	V99
IRAS 14348–1447	0.083	Paα $>$2500	N91	?	...	11.48	21.48	F03	4.53	41.89	V99
NGC 1386	0.0029	Brγ	R02	n	M00	3.74	$>$24	L06	1020	41.27	S89
NGC 7582	0.0052	Brγ3000	R03	n	H97	6.62	23.89	P07	369	41.36	S95
Mrk 463E	0.05	Paβ1794, Brγ1070	V97a	y	Y96	1.35	23.51	I04	125	42.89	D88
Mrk 477	0.038	Brγ1630	V97a	y	T92	2.71	$>$24	B99	1240	43.62	D88
NGC 2110	0.0078	Paβ1204, Brγ3127	V97a	y	M07	4.92	22.48	E07	321	41.62	B99
NGC 262, Mrk 348	0.015	Paβ1850, Brγ2500	V97a	y	D88	1.54	23.20	A00	177	41.96	D88
NGC 7674	0.029	Paα3000, Brγ3000	R06	y	Y96	2.79	$>$24	B05a	193	42.57	D88
F20460+1925	0.18	Paα2857	V97b	y	Y96	1.55	22.40	B99	11.2	43.02	B99
F23060+0505	0.17	Paα1954	V97b	y	D04	2.69	22.92	B07	99.45	43.92	B99
F05189–2524	0.042	Paα2619	V99	y	Y96	3.98	22.83	T09	130	42.74	L01
IRAS 11058–1131	0.055	Paα7179	V99	y	Y96	2.4	$>$24	U00	39.4	42.45	Y96
Mrk 3	0.014	...	H99	y	M90	1.34	24.13	B05b	4610	43.27	M94
Mrk 176	0.027	Paβ1329	R94	y	M83	2.96	23.88	G05	105	42.19	K78
PKS 1549–79	0.15	Paα1745	B03	y	S95	2.15	...	...	130	41.15	H06
3C 234	0.184	Paα4100	H96	y	Y98	0.89	23.54	Pi08	20.9	43.3	P08
NGC 1275	0.018	He I 1.08μm4700	R06	y	G01	2.11	21.08	C03	311	42.34	B99

Col. (1): the source name; Col. (2): the redshift; Col. (3): the width of NIR broad lines. The letters and number denote the type of lines and their velocities (in units of km s^{-1}), respectively; Col. (4): the references for the observations of near-infrared broad lines; Col. (5): whether they have been observed optically as polarized broad lines; Col. (6): the references for the observations of polarized broad lines; Col. (7): the ratio of the flux at 60 μm to the flux at 25 μm; Cols. (8) and (9): the hydrogen density by X-ray observations and their references, respectively; Cols. (10), (11) and (12): the reddening-corrected [O III] flux density (in units of 10^{-14} erg cm^{-2} s^{-1}), [O III] luminosity (in units of erg s^{-1}), and their references, respectively.

Ref. A00: Axon et al. (2000); A06: Awaki et al. (2006); B99: Bassani et al. (1999); B03 Bellamy et al. (2003); B07: Bian & Gu (2007); B05a: Bianchi et al. (2005a); B05b: Bianchi et al. (2005b); C02: Clements et al. (2002); C03: Churazov et al. (2003); C04: Croston et al. (2004); D88: Dahari & De Robertis (1988); D04: Deluit (2004); D87: DePoy et al. (1987); E07: Evans et al. (2007); F03: Franceschini et al. (2003); G01: Gu et al. (2001); G05: Guainazzi et al. (2005); H97: Heisler et al. (1997); H99: Heisler & De Robertis (1999); H96: Hill et al. (1996); H06: Holt et al. (2006); I04: Imanishi & Terashima (2004); K78: Koski (1978); L06: Levenson et al. (2006); L01: Lumsden et al. (2001); L02: Lutz et al. (2002); M83: Martin et al. (1983); M90: Miller & Goodrich (1990); M00: Moran et al. (2000); M94: Mulchaey et al. (1994); M99: Murphy et al. (1999); M00: Murphy et al. (2000); N91: Nakajima et al. (1991); N05: Netzer et al. (2005); P03: Ptak et al. (2003); P07: Piconcelli et al. (2007); Pi08: Piconcelli et al. (2008); P08: Privon et al. (2008); Reunanen et al. (2002); R03: Reunanen et al. (2003); R06: Riffel et al. (2006); R94: Ruiz et al. (1994); S08: Sani et al. (2008); S95: Storchi-Bergmann et al. (1995); S89: Storchi-Bergmann & Pastoriza (1989); T09: Teng et al. (2009); T01: Tran (2001); U00: Ueno et al. (2000); V97a: Velilleux et al. (1997a); V97b: Velilleux et al. (1997b); V99: Veilleux et al. (1999); W93: Warwick et al. (1993); Y96: Young et al. (1996); Y98: Young et al. (1998).

Table 2 Sample of Seyfert 2s without the Detection of Near-infrared Broad Lines

Source (1)	z (2)	Ref. (3)	PBL (4)	Ref. (5)	f_{60}/f_{25} (6)	$\log N_{\rm H}$ (7)	Ref. (8)	$F_{[\rm O\ III]}$ (9)	$\log L_{[\rm O\ III]}$ (10)	Ref. (11)
Mrk 273	0.038	V99	?	...	9.55	23.61	X02	84	42.44	B99
Mrk 1073	0.023	V97a	?	...	5.71	>24	G05	21.95	41.42	B97
F12072–0444	0.13	V97b	?	...	4.57	>24	T05	118.35	43.71	V99
Mrk 622	0.023	V97a	?	...	1.28	>24	G05	3.92	40.68	B97
NGC 4968	0.0099	L02	?	...	2.27	>24	L02	1116	42.38	B99
NGC 7172	0.0087	V97a	n	H97	6.64	22.95	S07	4.04	39.83	Va97
NGC 5643	0.0040	L02	n	M00	5.16	>25	L02	661.76	41.37	M94
NGC 1142	0.029	R06	n	T01	8.37	23.65	Sa07	38.82	41.87	V95
NGC 7130	0.016	V97a	n	H97	7.76	>24	L05	600	42.55	S95
NGC 34	0.020	R06	n	H97	6.96	>24	S07	768	42.83	V95
Mrk 266	0.028	V97a	n	T01	4.6	>25	R00	44	41.89	D88
NGC 4941	0.0037	L02	n	M00	2.61	23.65	L02	457	41.14	S89
ESO 428-G14	0.0057	V97a	n	M00	2.49	>24	L06	2010	42.15	A91
Mrk 78	0.037	V97a	n	M90	2	...	...	105.7	42.53	K78
Mrk 1	0.016	V97a	n	K78	2.93	>24	G05	55.04	41.5	N00
NGC 4945	0.0019	R02	n	M06	14.17	24.70	I08	>40	>39.48	R99
NGC 5728	0.0094	V97a	n	M00	9.24	23.91	Z06	761	42.18	S95
Mrk 1066	0.012	V97a	n	M00	4.77	23.95	G05	514	42	M94
F04103–2838	0.12	V99	n	Y96	3.39	>24	T08	21.34	42.88	V99
NGC 5128	0.0018	R02	n	A99	8.47	23.00	E04	>7	>38.73	B99
NGC 3081	0.007976	V97a	y	M00	...	23.82	B99	195	41.43	S95
NGC 5929	0.0083	R06	y	M01	5.64	...	S07	153	41.4	L01
NGC 4388	0.0084	V97a	y	Y96	2.7	23.32	C06	451	41.85	D88
NGC 1068	0.0038	V97a	y	A85	2.12	>24	P06	6780	42.33	D88
Mrk 573	0.017	V97a	y	N04	1.34	>24	G05	177	42.08	D88
Circinus	0.0014	L02	y	O98	3.63	24.60	L02	1848.6	40.92	L05
NGC 7212	0.027	V97a	y	T92	3.75	>24	G05	320	42.73	M94
Mrk 1157	0.015	V97a	y	M00	4.44	>24	G05	178	41.97	M94
Mrk 1210	0.014	L02	y	T92	0.91	23.26	O04	580	42.37	T91

Col. (1): the source name; Col. (2): the redshift; Col. (3): where the references for the observations of near-infrared broad lines; Col. (4): whether they have been observed optically as polarized broad lines; Col. (5): the references for the observations of polarized broad lines; Col. (6): the ratio of the flux at 60 μm to the flux at 25 μm; Cols. (7) and (8): the hydrogen density by X-ray observations, and their references, respectively; Cols. (9), (10) and (11): the reddening-corrected [O III] flux density (in units of 10^{-14} erg cm^{-2} s^{-1}), [O III] luminosity (in units of erg s^{-1}), and their references, respectively.

Ref. A91: Acker et al. (1991); A99: Alexander et al. (1999); A85: Antonucci & Miller (1985); B99: Bassani et al. (1999); B97: Bonatto & Pastoriza (1997); C06: Cappi et al. (2006); D88: Dahari & De Robertis (1988); D04: Deluit (2004); D03: Dennefeld et al. (2003); E04: Evans et al. (2004); G05: Guainazzi et al. (2005); H97: Heisler et al. (1997); I08: Itoh et al. (2008), PASJ; K78: Koski (1978); L05: Levenson et al. (2005); L06: Levenson et al. (2006); L01: Lumsden et al. (2001); L02: Lutz et al. (2002); M06: Madejski et al. (2006); M00: Moran et al. (2000); M01: Moran et al. (2001); M94: Mulchaey et al. (1994); N00: Nagao et al. (2000); N04: Nagao et al. (2004); O04: Ohno et al. (2004); O98: Oliva et al. (1998); P06: Pounds & Vaughan (2006); R06: Riffel et al. (2006); R99: Risaliti et al. (1999); R00: Risaliti et al. (2000); Sa07: Sazonov et al. (2007); S07: Shu et al. (2007); S89: Storchi-Bergmann & Pastoriza (1989); S95: Storchi-Bergmann et al. (1995); T05: Teng et al. (2005); T08: Teng et al. (2008); T91: Terlevich et al. (1991); T92: Tran et al. (1992); T01: Tran (2001); Va97: Vaceli et al. (1997); V95: Veilleux et al. 1995; V97a: Veilleux et al. (1997a); V97b: Veilleux et al. (1997b); V99: Veilleux et al. (1999); X02: Xia et al. (2002); Y96: Young et al. (1996); Z06: Zhang et al. (2006).

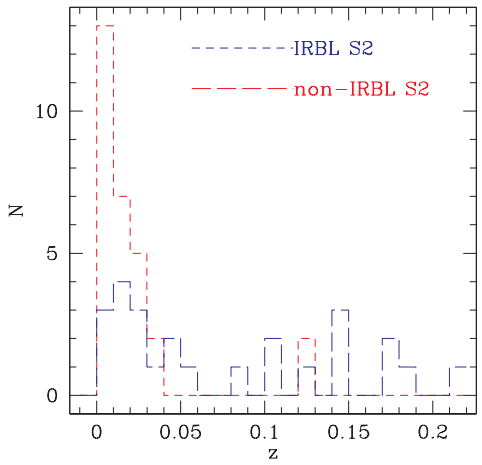

Fig. 1 Distribution of redshifts of IRBL S2s and non-IRBL S2s.

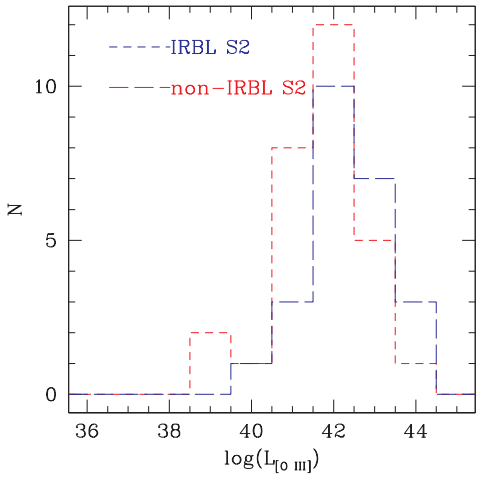

Fig. 2 Distribution of $L_{[\mathrm{O\ III}]}$ of IRBL S2s and non-IRBL S2s.

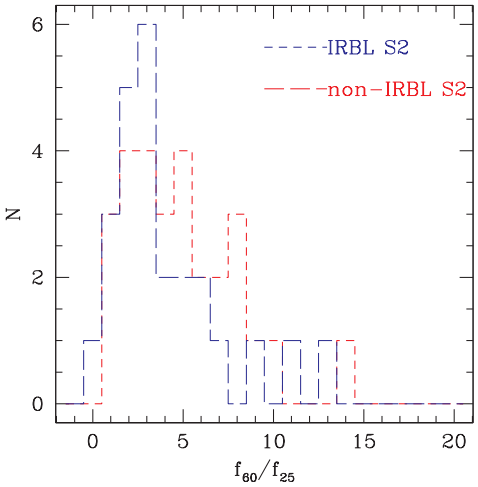

Fig. 3 Distributions of f_{60}/f_{25} of IRBL S2s and non-IRBL S2s.

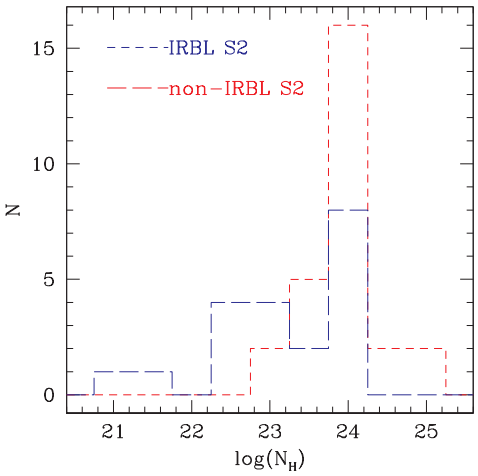

Fig. 4 Distribution of the hydrogen column densities of IRBL S2s and non-IRBL S2s.

Heisler et al. (1997) found that the visibility of PBLs is related to the far-infrared colors and Seyfert 2s with warmer FIR colors ($f_{60}/f_{25} < 4$) are more likely to have hidden broad lines. Here we also investigate whether the visibility of NIR broad lines in S2s depends on FIR colors. We plot the distributions of FIR colors ($f_{60\,\mu\mathrm{m}}/f_{25\,\mu\mathrm{m}}$) of IRBL S2s and non-IRBL S2s in Figure 3, and find no statistical difference between the two populations.

The X-ray absorption column densities were collected from the literature for two samples. Whenever available, we cite measurements based on Chandra/XMM data which have higher spatial resolution and higher spectral quality compared with previous data. In Figure 4 we plot the N_{H} distribution for IRBL S2s and non-IRBL S2s, where we can clearly see weaker X-ray obscuration in IRBL S2s. A K-S test shows that the difference in N_{H} between the two populations is significant at the 99% level.

3 DISCUSSION

3.1 IRBL S2s versus Non-IRBL S2s

Comparing our samples of IRBL S2s with non-IRBL S2s, we find that while IRBL S2s have a significantly higher redshift, their intrinsic AGN luminosity distribution is statistically consistent with non-IRBL S2s. The consequence is that the non-detection of infrared broad emission lines in non-IRBL S2s, which are located at even lower redshifts, is not likely due to the detection limit of IR spectral observations. The similar distribution of FIR colors (f_{60}/f_{25}) in the two populations and the smaller redshift in non-IRBL S2s (which suggests a smaller contribution from the host galaxy for a fixed slit width) also suggest that the non-detection of NIR broad emission lines could not be attributed to stronger host galaxy contamination.

Recent studies have suggested that the BLR might be absent in low luminosity and/or low accretion rate AGNs (e.g., Elitzur & Ho 2009). However, the consistent intrinsic AGN luminosity in IRBL S2s and non-IRBL S2s suggests that the non-detection of an NIR BLR in our sample was not due to the intrinsic absence of a BLR, but due to heavy obscuration.

Consistently, we find significantly higher X-ray obscuration in non-IRBL S2s, 66% of which are obscured with column density $> 10^{24}$ cm^{-2}, while the fraction for IRBL S2s is only 29%. This result is consistent with Lutz et al. (2002), who detected low X-ray absorption in IRBL S2s in a much smaller sample.

We also check the relation between the detection of the NIR broad emission line and that of the polarized broad emission line in Seyfert 2 galaxies. By matching our sample with spectropolarimetric observations in the literature (see Tables 1 and 2), we find that PBLs were detected in 14 out of 16 IRBL S2s with both NIR spectral and optical spectropolarimetric observations, but in a much smaller fraction (9 out of 24) of non-IRBL S2s. This suggests that the visibility of a BLR in NIR spectra and in polarized spectra is connected. Shu et al. (2007) found that S2s with PBLs have smaller X-ray obscuration. This pattern is consistent with our finding that S2s with NIR broad emission lines have lower X-ray obscuration.

3.2 Dust Extinction versus X-ray Obscuration

The optical dust extinction in AGNs (E_{B-V} or A_V) has been compared with X-ray obscuring column densities by many studies, which yield a rather large diversity in the observed dust-to-gas ratios. In particular, Maiolino et al. (2001a) reported that $E_{B-V}/N_{\rm H}$ appears ~ 3 to ~ 100 times lower than Galactic in various classes of AGNs, most of which are Seyfert 1s, quasars and intermediate Seyferts. Maiolino et al. (2001b) attributed the lower $E_{B-V}/N_{\rm H}$ to several possible mechanisms, including dust distribution dominated by large grains (their most favorable model), metallicity higher than solar which would affect $N_{\rm H}$ measurements through X-ray spectral fitting, low dust-to-gas ratio, geometry effect, etc. (also see Wang & Zhang 2007). On the other hand, dust-to-gas ratios consistent with or even much higher than the Galactic value were also reported. For instance, Wang et al. (2009) reported a dust-to-gas ratio consistent with the Galactic value in the partially obscured Seyfert galaxy Mrk 1393, while much higher dust-to-gas ratios were reported in some AGNs which could be due to ionized absorbers mixing with the dust (see Komossa 1999 for a review).

Taking the large diversity in the ratio of observed dust reddening to X-ray column density, we are not surprised to see a significant number of IRBL S2s with large X-ray obscuration (e.g. those with $N_{\rm H} > 10^{23}$ cm^{-2} in Fig. 4), which were absent from the small sample of Lutz et al. (2002). The possible mechanisms proposed by Maiolino et al. (2001b) could also apply here. We note that the samples we presented are not uniformly selected, since various NIR observations were designed to search for various NIR broad emission lines with different detection limits. A stricter comparison between the two populations requires direct measurements of NIR extinction for each detected NIR

broad emission line, and lower limits for those non-detected ones, most of which were unavailable, however, from the literature.

Nevertheless, the detection of IR broad emission lines in those X-ray Compton-thick S2s (with $N_{\rm H} > 10^{24}$ cm^{-2}) is still a puzzle, since the thick X-ray absorption is too large for the detection of NIR BLRs (e.g. the detection of Brα implying $N_{\rm H} < 10^{23}$ cm^{-2} assuming a Galactic extinction curve, see Lutz et al. 2002). The discrepancy cannot be solved even assuming a dust-to-gas ratio 10 times lower than the Galactic value. Dust dominated by large grains could not help either since dust with large grains has a much flatter extinction curve, and does not significantly alter the opacity in NIR (see fig. 5 of Lutz et al. 2002).

3.3 IR-thin X-ray-thick S2s and their Spectral Transitions

For the six IRBL S2s identified as Compton-thick in X-ray (NGC 1386, NGC 7674, Mrk 3, NGC 6240, Mrk 477, and IRAS 11058–1131), we hereafter refer to them as IR-thin X-ray-thick Seyfert 2 galaxies. Below, we discuss several possible explanations for the discrepancy between the detection of NIR broad lines and Compton-thick X-ray obscuration.

From the viewpoint of the traditional unification model, this discrepancy can be ascribed to the different emission regions of broad emission lines and the X-ray continuum. These sources could be viewed along the edge of the torus where the absorption is along the line of sight with respect to the central engine, which is still X-ray thick, while that to the outer part of a BLR at larger distances has a much lower column density. In this scheme, the column density of the torus smoothly decreases from edge-on to face-on, and these sources (infrared-thin X-ray thick) can only be detected at intermediate inclination angles.

However, the geometry of the torus in an AGN is still unclear. The recent view of the unification model has suggested that the obscuring torus is most likely clumpy instead of smoothly distributed. The evidence comes, for instance, from the IR SED fitting (e.g. Ramos Almeida et al. 2009), and the detection of rapid variation of X-ray absorption in Seyfert 2 galaxies (e.g. Risaliti et al. 2007). In this model, it is much easier to understand the observed different opacities detected in the IR and X-ray bands: we could expect that a BLR is mainly obscured by a Compton-thin medium, with clumpy Compton-thick clouds mixing within it. The typical size of a single Compton-thick cloud must be much smaller than a BLR, otherwise one would see consistent $N_{\rm H}$ inferred from optical/NIR and from X-ray. Nevertheless, considering that NIR BLRs have been detected only in a small fraction of Compton-thick S2s, IR-thin/X-ray-thick S2s must be viewed differently from those IR-thick/X-ray-thick ones. Compared with IR-thick X-ray-thick sources, they could be at a certain evolution stage or at an intermediate inclination angle when/where the clumpy Compton-thick clouds do exist to block the central X-ray continuum with a certain probability, but with filling factors which are too small to block the whole BLR. In Figure 5 we present a cartoon diagram to demonstrate the toy model we propose. If the model is right, we would expect X-ray absorption variations in these IR-thin X-ray thick Seyfert 2 galaxies, due to the movement of the compact Compton-thick clouds.

Alternatively, the discrepancy could be to due to the fact that IR and X-ray observations were not obtained simultaneously. For instance, sources with fading central engines might be mis-classified as Compton-thick against their Compton-thin nature, because the observed X-ray spectra could be dominated by a reflection component on a much larger scale due to the fading of the direct emission (e.g. Matt et al. 2003).

Both of the latter two models which we presented above predict or require spectral transitions (i.e. from Compton-thin to Compton-thick or vice versa) for our IR-thin X-ray-thick S2s. By searching previous X-ray observations, we found X-ray spectral transitions in two out of six IR-thin X-ray-thick S2s (NGC 1386 and NGC 7674).

Risaliti et al. (2002) have studied NGC 1386 in X-ray and found that it changed from Compton-thin ($N_{\rm H}$ = 2.8 $\times$ 10^{23} cm^{-2}) on 1995 Jan 25, to Compton-thick on 1996 Dec 10, which means that

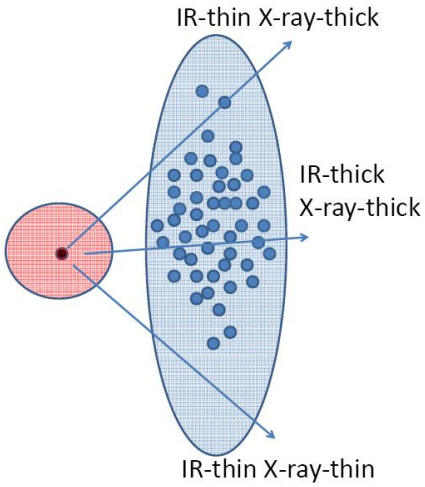

Fig. 5 A cartoon diagram demonstrates why we see IR-thin X-ray-thick S2s, and why they are special. While we observe the central X-ray source (*plotted as a black dot*) through the dusty medium (*large blue region*, see electronic version) without the intervening Compton-thick clouds (*blue dots*), we see them as IR-thin/X-ray-thin, otherwise as IR-thin/X-ray-thick. In the situation that the density (or sky coverage) of the Compton-thick clouds are high enough that most of the BLR (*red region*) could be blocked by the Compton-thick clouds, we see them as IR-thick/X-ray-thick. In addition, such situations as these might be an evolution effect, instead of an inclination effect as shown in this cartoon, i.e., the torus evolves with time, and the appearance of S2s depends on the evolving status of the torus, instead of the inclination angle.

the timescale of variation is less than 2 yr. This source likely remained Compton-thick till the XMM observation in Dec. 2002 (Guainazzi et al. 2005).

Bianchi et al. (2005) reported that the hard X-ray flux density of NGC 7674 decreased from 24×10^{-12} erg cm^{-2} s^{-1} in 1977 (HEAO A-1) to 8×10^{-12} erg cm^{-2} s^{-1} in 1989 (GINGA). BeppoSAX in 1996 and XMM-Newton in 2004 also observed this source, with a much smaller hard X-ray flux density of 0.75 and 0.70×10^{-12} erg cm^{-2} s^{-1}, respectively. Bianchi et al. also presented a spectral transition between GINGA observations (1989) and BeppoSAX/XMM-Newton observations, from transmission-dominated to reflection-dominated. They argued that it was likely due to the "switching-off" of the central engine in NGC 7674, and the reflection-dominated spectra observed by BeppoSAX and XMM are the delayed emission (with an 8$\sim$15 yr delay) from a reflector at a larger distance (such as the inner surface of a torus) although they cannot rule out the variation of the absorption column density. Here we argue that the transition is more likely due to the variation in absorption based on two reasons: 1) the size of the inner torus radius in Seyfert galaxies is believed to be within several light weeks to several light months (see Suganuma et al. 2006), much smaller than that derived based on X-ray transition (8$\sim$15 yr); this means the delayed reflection emission should disappear several months after "switching-off" and cannot last 8$\sim$15 yr; 2) the broad emission line, which is produced at an even smaller distance than the torus and should disappear even faster after "switching-off," was detected in near-IR 6 yr after the so-called "switching-off" (Riffel et al. 2006).

No X-ray transitions were reported in the remaining four IR-thin X-ray-thick S2s. Note that Turner et al. (1997) and Awaki et al. (2000) both reported the variability of hard X-ray flux in Mrk 3 within one year. More interestingly, a recent Suzaku observation (Ikeda et al. 2009) suggested Mrk 3 is viewed at a particular inclination (along the edge of the torus). For NGC 6240, no X-ray transition

is observed though there was a flux variability with a factor of $\sim$ 1.7 from 1994 to 1998 (Ptak et al. 2003). Note that NGC 6240 is well known because it contains a binary active galactic nucleus (Komossa et al. 2003). For Mrk 477 and IRAS 11058–1131, X-ray observations are rather limited. The available X-ray spectral parameters are from ASCA and BeppoSAX from about 20 yr ago for Mrk 477 and IRAS 11058–1131, respectively (Bassani et al. 1999; Risaliti et al. 2000).

We finally propose, based on our toy model and the above observational evidence, that IR-thin X-ray-thick S2s are a special type of X-ray-thick S2s. They can be viewed at an intermediate angle (i.e., along the edge of the Compton-thick torus) compared with IR-thick X-ray-thick S2s, and might have a higher rate of producing spectral transitions than other X-ray thick S2s. We note that Guainazzi et al. (2005) detected only one transition out of 11 optically selected Compton-thick AGNs. Following up or monitoring observations of this particular class of sources could give valuable information on obscuration in AGNs.

Acknowledgements H.Cai gratefully acknowledges the support of the K. C. Wong Education Foundation, Hong Kong, and the China Postdoctoral Science Foundation No. 20080430769. The work was supported by the National Natural Science Foundation of China (Grant Nos. 10773010 and 10825312), and the Knowledge Innovation Program of CAS (Grant No. KJCX2-YW-T05).

References

Acker, A., Stenholm, B., & Veron, P. 1991, A&AS, 87, 499
Alexander, D. M., Hough, J. H., Young, S., Bailey, J. A., Heisler, C. A., Lumsden, S. L., & Robinson, A. 1999, MNRAS, 303, L17
Antonucci, R., & Miller, J. S. 1985, ApJ, 297, 621
Antonucci, R. R. J. 1993, ARA&A, 31, 473
Awaki, H., Ueno, S., Taniguchi, Y., & Weaver, K. A. 2000, ApJ, 542, 175
Axon, D. J., Capetti, A., Fanti, R., Morganti, R., Robinson, A., & Spencer, R. 2000, AJ, 120, 2284
Bassani, L., Dadina, M., Maiolino, R., Salvati, M., Risaliti, G., della Ceca, R., Matt, G., & Zamorani, G. 1999, ApJS, 121, 473
Bellamy, M. J., Tadhunter, C. N., Morganti, R., Wills, K. A., Holt, J., Taylor, M. D., & Watson, C. A. 2003, MNRAS, 344, L80
Bian, W., & Gu, Q. 2007, ApJ, 657, 159
Bianchi, S., et al. 2005a, A&A, 422, 185
Bianchi, S., Miniutti, G., Fabian, A., & Iwasawa, K. 2005b, MNRAS, 360, 380
Bianchi, S., Corral, A., Panessa, F., Barcons, X., Matt, G., et al. 2008, MNRAS, 385, 195
Bonatto, C. J., & Pastoriza, M. G. 1997, ApJ, 486, 132
Cappi, M., Panessa, F., Bassani, L., et al. 2006, A&A, 446, 459,
Churazov, E., Forman, W., Jones, C., & Bohringer, H. 2003, ApJ, 590, 225
Clements, D. L., et al. 2002, ApJ, 581, 974
Croston, J. H., et al. 2004, MNRAS, 353, 879
Dahari, O., & De Robertis, M. M. 1988, ApJS, 67, 249
Deluit, S. J. 2004, A&A, 415, 39
Dennefeld, M., Boller, T., Rigopoulou, D., & Spoon, H. W. W. 2003, A&A, 406, 527
DePoy, D. L., Becklin, E. E., & Geballe, T. R. 1987, ApJ, 316, L63
Elitzur, M., & Ho, L. C. 2009, ApJ, 701, L91
Evans, D. A., et al. 2004, ApJ, 612, 786
Evans, D. A., et al. 2007, ApJ, 671, 1345
Franceschini, A., et al. 2003, MNRAS, 343, 1181
Goodrich, R. W., Veilleux, S., & Hill, G. J. 1994, ApJ, 422, 521

Gordon, K. D., et al. 2003, ApJ, 594, 279
Gu, Q., Dultzin-Hacyan, D., & de Diego, J. A. 2001, Revista Mexicana de Astronomia y Astrofisica, 37, 3
Guainazzi, M., Matt, G., & Perola, G. C. 2005, A&A, 444, 119
Heisler, C. A., Lumsden, S. L., & Bailey, J. A. 1997, Nature, 385, 700
Heisler, C. A., & De Robertis, M. M. 1999, AJ, 118, 2038
Hill, G. J., Goodrich, R. W., & DePoy, D. L. 1996, ApJ, 462, 163
Holt, J., Tadhunter, C., Morganti, R., Bellamy, M., Gonzalez Delgado, R. M., Tzioumis, A., & Inskip, K. J. 2006, MNRAS, 370, 1633
Ikeda, S., Awaki, H., & Terashima, Y. 2009, ApJ, 692, 608
Imanishi, M., & Terashima, Y. 2004, AJ, 127, 758
Itoh, T., et al. 2008, 60, 251, PASJ
Komossa, S. 1999, ASCA-ROSAT Workshop on AGN, eds. T. Takahashi, & H. Inoue (ISAS Report 149; Tokyo: ISAS), 149
Komossa, S., et al. 2003, ApJ, 582, L15
Koski, A. T. 1978, ApJ, 223, 56
Levenson, N. A., Weaver, K. A., Heckman, T. M., Awaki, H., & Terashima, Y. 2005, ApJ, 618, 167
Levenson, N. A., Heckman, T. M., Krolik, J. H., Weaver, K. A., & Życki, P. T. 2006, ApJ, 648, 111
Lumsden, S. L., Heisler, C. A., Bailey, J. A., Hough, J. H., & Young, S. 2001, MNRAS, 327, 459
Lutz, D. 1999, The Universe as seen by ISO, eds. P. Cox, & M. F. Kessler (ESA-SP), 427, 623
Lutz, D., Maiolino, R., Moorwood, A. F. M., Netzer, H., & Wagner, S. J. 2002, A&A, 396, 439
Madejski, G., Done, C., Życki, P. T., & Greenhill, L. 2006, ApJ, 636, 75
Maiolino, R., et al. 2001a, A&A, 365, 28
Maiolino, R., Marconi, A., & Oliva, E. 2001b, A&A, 365, 37
Martin, P. G., Thompson, I. B., Maza, J., & Angel, J. R. P. 1983, ApJ, 266, 470
Matt, G., Guainazzi, M., & Maiolino, R. 2003, MNRAS, 342, 422
Miller, J. S., & Goodrich, R. W. 1990, ApJ, 355, 456
Moran, E. C., Barth, A. J., Kay, L. E., & Filippenko, A. V. 2000, ApJ, 540, L73
Moran, E. C., Kay, L. E., Davis, M., Filippenko, A. V., & Barth, A. J. 2001, ApJ, 556, L75
Mulchaey, J. S., Koratkar, A., Ward, M. J., Wilson, A. S., Whittle, M., Antonucci, R. R. J., Kinney, A. L., & Hurt, T. 1994, ApJ, 436, 586
Murphy, T. W. Jr., Soifer, B. T., Matthews, K., Kiger, J. R., & Armus, L. 1999, ApJ, 525, L85
Murphy, T. W. Jr., Soifer, B. T., Matthews, K., & Armus, L. 2000, AJ, 120, 1675
Nagao, T., Taniguchi, Y., & Murayama, T. 2000, AJ, 119, 2605
Nagao, T., Kawabata, K. S., Murayama, T., Ohyama, Y., Taniguchi, Y., Shioya, Y., Sumiya, R., & Sasaki, S. S. 2004, AJ, 128, 2066
Nakajima, T., Kawara, K., Nishida, M., & Gregory, B. 1991, ApJ, 373, 452
Netzer, H., Lemze, D., Kaspi, S., George, I. M., Turner, T. J., Lutz, D., Boller, T., & Chelouche, D. 2005, ApJ, 629, 739
Ohno, M., Fukazawa, Y., & Iyomoto, N. 2004, PASJ, 56, 425
Oliva, E., Marconi, A., Cimatti, A., & Alighieri, S. D. 1998, A&A, 329, L21
Piconcelli, E., et al. 2007, A&A, 466, 855
Piconcelli, E., Bianchi, S., Miniutti, G., Fiore, F., Guainazzi, M., Jimenez-Bailon, E., & Matt, G. 2008, A&A, 480, 671
Pounds, K., & Vaughan, S. 2006, MNRAS, 368, 707
Privon, G. C., O'Dea, C. P., Baum, S. A., Axon, D. J., Kharb, P., Buchanan, C. L., Sparks, W., & Chiaberge, M. 2008, ApJS, 175, 423
Ptak, A., Heckman, T., Levenson, N. A., Weaver, K., & Strickland, D. 2003, ApJ, 592, 782
Ramos Almeida, C., et al. 2009, ApJ, 702, 1127

Reunanen J., Kotilainen J. K., & Prieto, M. A. 2002, MNRAS, 331, 154
Reunanen J., Kotilainen J. K., & Prieto, M. A. 2003, MNRAS, 343, 192
Riffel, R., Rodríguez-Ardila, A., & Pastoriza, M. G. 2006, A&A, 457, 61
Risaliti, G., Maiolino, R., & Salvati, M. 1999, ApJ, 522, 157
Risaliti, G., Gilli, R., Maiolino, R., & Salvati, M. 2000, A&A, 357, 13
Risaliti, G., Elvis, M., & Nicastro, F. 2002, ApJ, 571, 234
Risaliti G., Elvis M., Fabbiano G., Baldi A., Zezas A., et al. 2007, ApJ, 659, L111
Ruiz, M., Rieke, G. H., & Schmidt, G. D. 1994, ApJ, 423, 608
Sani, E., Risaliti, G., Salvati, M., et al. 2008, ApJ, 675, 96
Suganuma, M., et al. 2006, ApJ, 639, 46
Sazonov, S., Revnivtsev, M., Krivonos, R., Churazov, E., & Sunyaev, R. 2007, A&A, 462, 57
Shu, X. W., Wang, J. X., Jiang, P., Fan, L. L., & Wang, T. G. 2007, ApJ, 657, 167
Storchi-Bergmann, T., & Pastoriza, M. G. 1989, ApJ, 347, 195
Storchi-Bergmann, T., Kinney, A. L., & Challis, P. 1995, ApJS, 98, 103
Teng, S. H., Wilson, A. S., Veilleux, S., Young, A. J., Sanders, D. B., & Nagar, N. M. 2005, ApJ, 633, 664
Teng, S. H., et al. 2008, ApJ, 674, 133
Teng, S. H., et al. 2009, ApJ, 691, 261
Terlevich, R., Melnick, J., Masegosa, J., Moles, M., & Copetti, M. V. F. 1991, A&AS, 91, 285
Tran, H. D., Miller, J. S., & Kay, L. E. 1992, ApJ, 397, 452
Tran, H. D. 2001, ApJ, 554, L19
Turner, T. J., George, I. M., Nandra, K., & Mushotzky, R. F. 1997, ApJ, 488, 164
Ueno, S., Ward, M. J., O'Brien, P. T., Stirpe, G. M., & Matt, G. 2000, AdSpR, 25, 823
Vaceli, M. S., Viegas, S. M., Gruenwald, R., & de Souza, R. E. 1997, AJ, 114, 1345
Veilleux, S., Kim, D.-C., Sanders, D. B., Mazzarella, J. M., & Soifer, B. T. 1995, ApJS, 98, 171
Veilleux, S., Goodrich, R. W., & Hill, G. J. 1997a, ApJ, 477,631
Veilleux, S., Sanders, D. B., & Kim, D. -C. 1997b, ApJ, 484, 92
Veilleux, S., Sanders D. B., & Kim, D.-C. 1999, ApJ, 522, 139
Wang, T. G., et al. 2009, AJ, 137, 4002
Wang, J. M., & Zhang, E. P. 2007, ApJ, 660, 1072
Warwick, R. S., Sembay, S., Yaqoob, T., Makishima, K., Ohashi, T., Tashiro, M., & Kohmura, Y. 1993, MNRAS, 265, 412
Xia, X. Y., Xue, S. J., Mao, S., Boller, Th., Deng, Z. G., & Wu, H. 2002, ApJ, 564, 196
Young, S., Hough, J. H., Efstathiou, A., Wills, B. J., Bailey, J. A., Ward, M. J., & Axon, D. J. 1996, MNRAS, 281, 1206
Young, S., Hough, J. H., Axon, D. J., Fabian, A. C., & Ward, M. J. 1998, MNRAS, 294, 478
Zhang, J. S., Henkel, C., Kadler, M., Greenhill, L. J., Nagar, N., Wilson, A. S., & Braatz, J. A. 2006, A&A, 450, 933